

UC Berkeley

UC Berkeley Previously Published Works

Title

Comprehensive Assessment of Osteoporosis and Bone Fragility with CT Colonography

Permalink

<https://escholarship.org/uc/item/659936s2>

Journal

Radiology, 278(1)

ISSN

0033-8419

Authors

Fidler, Jeff L
Murthy, Naveen S
Khosla, Sundeep
et al.

Publication Date

2016

DOI

10.1148/radiol.2015141984

Peer reviewed

Comprehensive Assessment of Osteoporosis and Bone Fragility with CT Colonography¹

Jeff L. Fidler, MD
Naveen S. Murthy, MD
Sundeep Khosla, MD
Bart L. Clarke, MD
David H. Bruining, MD
David L. Kopperdahl, PhD
David C. Lee, PhD
Tony M. Keaveny, PhD

An earlier incorrect version of this article appeared online. This article was corrected on July 24, 2015.

¹ From the Department of Radiology (J.L.F., N.S.M.), Division of Endocrinology (S.K., B.L.C.), and Division of Gastroenterology and Hepatology (D.H.B.), Mayo Clinic, 200 1st Ave SW, Rochester, MN 55902; O.N. Diagnostics, Berkeley, Calif (D.L.K., D.C.L., T.M.K.); and Departments of Mechanical Engineering and Bioengineering, University of California–Berkeley, Berkeley, Calif (T.M.K.). From the 2012 RSNA Annual Meeting. Received August 19, 2014; revision requested December 13; revision received March 24, 2015; accepted April 7; final version accepted May 14. Supported in part by O.N. Diagnostics. **Address correspondence to** J.L.F. (e-mail: fidler.jeff@mayo.edu).

© RSNA, 2015

Purpose:

To evaluate the ability of additional analysis of computed tomographic (CT) colonography images to provide a comprehensive osteoporosis assessment.

Materials and Methods:

This Health Insurance Portability and Accountability Act-compliant study was approved by our institutional review board with a waiver of informed consent. Diagnosis of osteoporosis and assessment of fracture risk were compared between biomechanical CT analysis and dual-energy x-ray absorptiometry (DXA) in 136 women (age range, 43–92 years), each of whom underwent CT colonography and DXA within a 6-month period (between January 2008 and April 2010). Blinded to the DXA data, biomechanical CT analysis was retrospectively applied to CT images by using phantomless calibration and finite element analysis to measure bone mineral density and bone strength at the hip and spine. Regression, Bland-Altman, and reclassification analyses and paired *t* tests were used to compare results.

Results:

For bone mineral density T scores at the femoral neck, biomechanical CT analysis was highly correlated ($R^2 = 0.84$) with DXA, did not differ from DXA ($P = .15$, paired *t* test), and was able to identify osteoporosis (as defined by DXA), with 100% sensitivity in eight of eight patients (95% confidence interval [CI]: 67.6%, 100%) and 98.4% specificity in 126 of 128 patients (95% CI: 94.5%, 99.6%). Considering both the hip and spine, the classification of patients at high risk for fracture by biomechanical CT analysis—those with osteoporosis or “fragile bone strength”—agreed well against classifications for clinical osteoporosis by DXA (T score ≤ -2.5 at the hip or spine), with 82.8% sensitivity in 24 of 29 patients (95% CI: 65.4%, 92.4%) and 85.7% specificity in 66 of 77 patients (95% CI: 76.2%, 91.8%).

Conclusion:

Retrospective biomechanical CT analysis of CT colonography for colorectal cancer screening provides a comprehensive osteoporosis assessment without requiring changes in imaging protocols.

©RSNA, 2015

Online supplemental material is available for this article.

Despite the clinical importance of osteoporosis and the growing size of the elderly population, about 70% of eligible women and far more men do not undergo bone mineral density (BMD) screening with dual-energy x-ray absorptiometry (DXA), the clinical standard (1,2). While the reasons for the underutilization of DXA are

unclear, reduced reimbursement rates in the United States limit access to DXA, and some patients may be reluctant to undergo a specific imaging procedure to screen for a condition that typically produces no symptoms (2,3). Thus, many patients who are recommended for osteoporosis screening but who go untested could benefit from the availability of an alternative test that is at least as safe and effective as DXA, is inexpensive, and can be performed on previously acquired imaging data without the need for additional examinations or radiation exposure (4,5). One such option is to analyze the bone in a computed tomographic (CT) examination that was originally performed for another clinical indication, potentially exploiting the millions of CT examinations performed each year in patients who meet osteoporosis screening criteria (6–8). While such approaches have been proposed to identify patients who should be recommended for DXA, we report here on a more comprehensive test that is termed biomechanical CT analysis and provides DXA-equivalent measurements of BMD and T scores at the hip and of vertebral trabecular BMD at the spine to directly identify patients with osteoporosis who are at high risk for fracture (9–13). In addition, biomechanical CT analysis can be used to identify patients without osteoporosis according to BMD criteria who have clinically important low levels of “fragile” bone strength as estimated by finite element analysis and are at high risk for fracture (14). Previously, we reported on this test as successfully applied to CT enterography for patients with inflammatory bowel disease (15). However, such procedures use intravenous contrast material, which prevents application of the test to the spine. Overcoming that limitation, the purpose of this study was to retrospectively

evaluate the ability of additional analysis of CT colonography to provide a comprehensive osteoporosis assessment.

Advances in Knowledge

- Clinical computed tomographic (CT) colonography images can be further analyzed to provide a comprehensive assessment of osteoporosis without requiring any change to the imaging protocol.
- Biomechanical CT analysis provides measures of bone mineral density (BMD) at the femoral neck that agree well ($R^2 = 0.84$) with those from dual-energy x-ray absorptiometry (DXA), with high sensitivity (100%; 95% confidence interval [CI]: 67.6, 100) in eight of eight patients and high specificity (98.4%; 95% CI: 94.5, 99.6) in 126 of 128 patients for classifying osteoporosis at the femoral neck.
- Biomechanical CT analysis provides measures of vertebral trabecular BMD at the spine that overcome projection artifacts, which were associated with aortic calcification (in 48 of 135 patients [35.6%]), osteophytes (in 11 of 135 patients [8.1%]), and facet degeneration (in three of 135 patients [2.2%]) at the L1 level.
- Considering both the hip and spine, classification of patients at high risk for fracture at biomechanical CT analysis agrees well with classifications of clinical osteoporosis at dual-energy x-ray absorptiometry (T-score ≤ -2.5 at the femoral neck, total hip, or lumbar spine), with high sensitivity (82.8%; 95% CI: 65.4, 92.4) in 24 of 29 patients and high specificity (85.7%; 95% CI: 76.2, 91.8%) in 66 of 77 patients.

Implication for Patient Care

- Biomechanical CT analysis of CT colonography can provide a comprehensive assessment of osteoporosis without requiring any change to the CT protocol.



Materials and Methods

Study Overview

Grant support for this study was provided by O.N. Diagnostics for the effort required to deidentify and electronically transfer data. Two authors (D.L.K. and D.C.L.) are employees of O.N. Diagnostics and performed image analysis. Initial statistical analysis was also performed at O.N. Diagnostics (T.M.K.). The authors who are not employees of or consultants for O.N. Diagnostics (J.L.F., N.S.M., S.K., B.L.C. and D.H.B.) had control of the inclusion of any data or information that might present a conflict of interest for those authors who are employees of or consultants for said industry.

This Health Insurance Portability and Accountability Act-compliant retrospective study was approved by our local institutional review board with a waiver of informed consent. All patients who were included in this study previously provided written approval

Published online before print

10.1148/radiol.2015141984 Content codes:  

Radiology 2016; 278:172–180

Abbreviations:

BMD = bone mineral density
CI = confidence interval
DXA = dual-energy x-ray absorptiometry

Author contributions:

Guarantors of integrity of entire study, J.L.F., D.H.B., D.C.L., T.M.K.; study concepts/study design or data acquisition or data analysis/interpretation, all authors; manuscript drafting or manuscript revision for important intellectual content, all authors; approval of final version of submitted manuscript, all authors; agrees to ensure any questions related to the work are appropriately resolved, all authors; literature research, J.L.F., B.L.C., D.C.L., T.M.K.; clinical studies, J.L.F., N.S.M., S.K., B.L.C., D.H.B., D.C.L.; experimental studies, D.C.L.; statistical analysis, D.H.B., D.C.L., T.M.K.; and manuscript editing, all authors

Funding:

This research was supported by the National Institutes of Health (grant AR057616).

Conflicts of interest are listed at the end of this article.

for use of their medical records for research purposes.

Patients

CT colonography images were retrieved for a consecutive series of women undergoing colorectal cancer screening between January 2008 and April 2010 ($n = 527$) who underwent hip DXA within 6 months of CT colonography (range, ± 167 days; $n = 210$). Patients with a body mass index greater than 30 ($n = 57$) or a metal implant at the hip or lumbar spine ($n = 17$) were excluded. A body mass index greater than 30 was chosen for exclusion to prevent potential inaccuracies in results that can occur with DXA in patients with high body mass index. Patients were not excluded on the basis of race, although all participants were white. This study focused on women, who have a higher rate of osteoporotic fracture than men, and the sample size was targeted to exceed that used in a comparable study ($n = 91$ women), in which a statistically rigorous paired comparison between DXA and quantitative CT-based BMD measurements at the hip was performed (16). Altogether, 136 women were selected for analysis (mean age, 68.5 years ± 10.1 ; range, 43–92 years; body mass index, 24.1 kg/m² ± 3.2). The available medical records indicated that, of these women, 62 were undergoing medical therapy (hormone, $n = 19$; tamoxifen, $n = 1$; raloxifene, $n = 5$; bisphosphonates, $n = 37$) for osteoporosis at the time CT colonography was performed. Five women were on medication that may promote bone loss (steroids, $n = 3$; aromatase-inhibitor, $n = 2$).

CT Imaging

Patients underwent standard CT colonography preparation, including fluid and stool tagging (17). All CT colonography images save one were acquired with the same imager (Lightspeed Pro 16; GE Healthcare, Milwaukee, Wis) by using 120 kVp and a patient size-adjusted tube current (mean, 64.1 mAs ± 17.0 ; range, 27–168 mAs). Images extended from above the splenic flexures to just below the pubic symphysis and were reconstructed with at least a 40-cm field of view, 1-mm spacing, and the

standard reconstruction kernel. For supine acquisitions, mean dose estimates were as follows: volume CT dose index, 6.8 mGy ± 3.5 ; dose-length product, 298 mGy \cdot cm ± 155 ; effective diameter, 27.5 cm ± 2.5 ; and size-specific dose estimate, 9.1 mGy ± 4.5 .

DXA-based BMD Analysis

For the DXA-based BMD measurements, standard clinical DXA images were obtained with five different Lunar DXA machines (GE Healthcare, Madison, Wis). While a hip DXA examination was performed in all patients ($n = 136$), a spine DXA examination was available for only a subset ($n = 107$). The main DXA outcomes were the BMD T scores (in the femoral neck, total hip, and, when available, total lumbar spine).

Biomechanical CT-BMD Analysis

All biomechanical CT analyses were blinded to DXA results with VirtuOst software (O.N. Diagnostics, Berkeley, Calif) and remotely conducted on deidentified Digital Imaging And Communications in Medicine (DICOM) images at O.N. Diagnostics (Appendix E1 [online]). For BMD measurements, each supine CT colonography image was calibrated to convert image attenuation values into units of BMD by using a phantomless approach that was developed prior to this study in which air, fat, and/or blood was used as an internal reference on a patient-specific basis (15). After calibration, the left hip and L1 vertebra were further processed, image quality and bone morphologic characteristics permitting (otherwise, the right hip or the L2 or L3 vertebra was analyzed). For the hip, biomechanical CT analysis returns Hologic (Bedford, Mass)-equivalent values of BMD (in g/cm³) and T scores by using automatically generated regions of interest for the femoral neck and total hip (Fig 1) (14,15). Because DXA-measured BMD at the spine is often confounded by various types of degenerative changes, instead of measuring a DXA-like BMD for the total spine region, biomechanical CT analysis measures the more robust vertebral trabecular density (in mg/cm³) (14,18–20).

Biomechanical CT-Bone Strength Analysis

By using the calibrated and segmented images, finite element models of the proximal femur and vertebral body were generated for each patient, a process that is described elsewhere (Fig 1) (21–23). Nonlinear finite element analysis was performed to virtually load bones to failure in a virtual stress test to measure whole-bone strength (in Newtons), simulating a sideways fall to the trochanter for the hip and a uniform compressive overload for the spine.

After completing all BMD and finite element analyses, one technician at O.N. Diagnostics who was blinded to DXA results qualitatively reviewed all CT images ($n = 135$) to quantify the prevalence of any aortic calcification, osteophytes, or obvious facet degeneration, each of which was assessed at only the single vertebral level for which the biomechanical CT analysis was performed (or at the L1 level). Statistical analysis was performed at O.N. Diagnostics and reviewed by an independent statistician at the Mayo Clinic. The main BMD outcome was the femoral neck BMD T score, which was directly compared between DXA and biomechanical CT analysis with linear regression and Bland-Altman analysis and a paired t test (BMD T-scores were compared, as opposed to BMD values, since Hologic and Lunar DXA imagers report slightly different BMD values but more consistent BMD T scores) (24,25). Paired t tests were used to detect any significant bias, and the 95% limits of agreement were taken as ± 1.96 times the standard deviation of the differences, centered about either zero or any significant ($P < .05$) bias.

The diagnostic equivalence of DXA and biomechanical CT analysis was assessed assuming DXA as the reference standard. For DXA, we compiled two classifications: osteoporosis (T score ≤ -2.5) at the femoral neck and osteoporosis at the femoral neck, total hip, or total lumbar spine (average of L1–L4). The former presents a focus on hip fracture assessment since the femoral neck T score is the preferred site for such assessment and is recommended for use in the World Health Organization

Figure 1

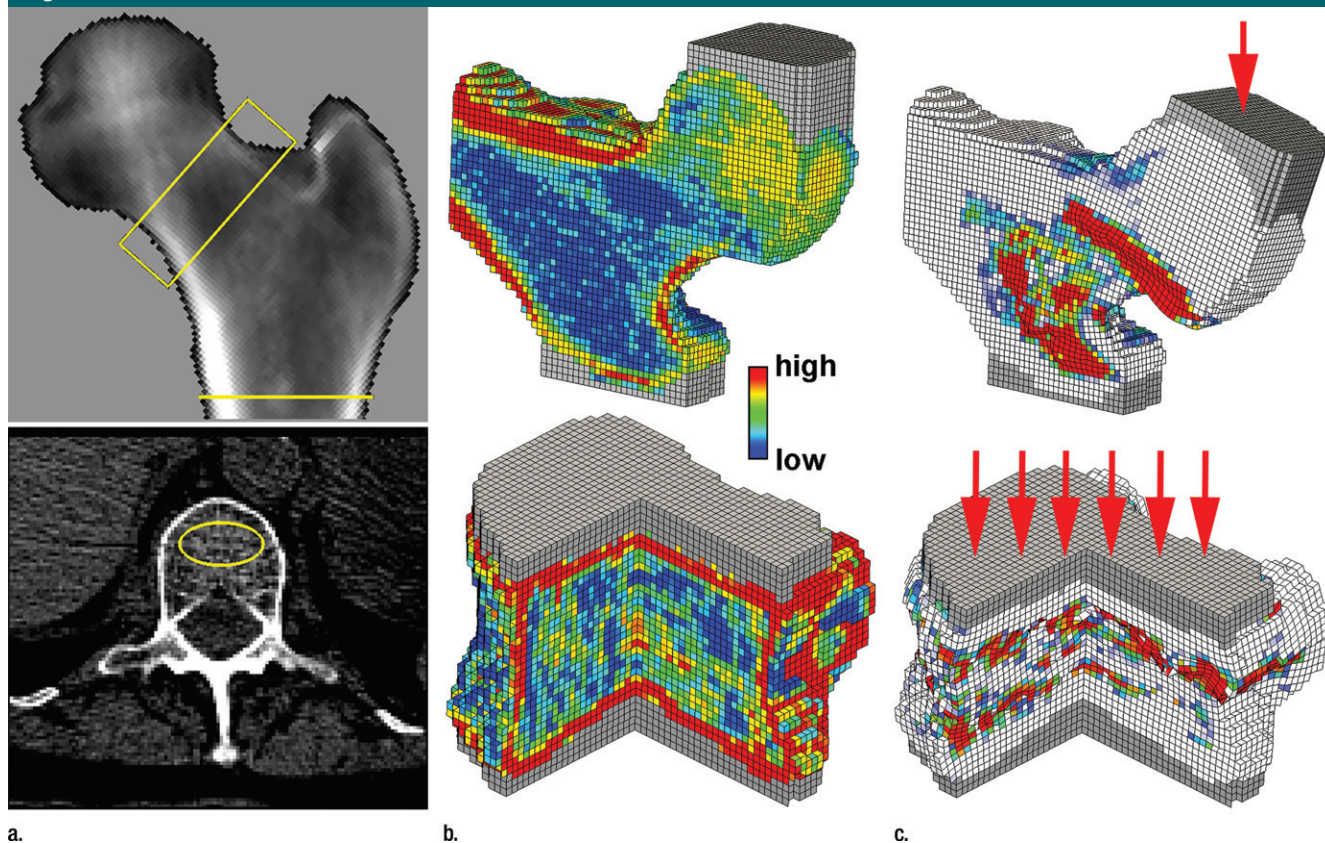


Figure 1: Biomechanical CT analysis of the hip and spine with CT colonography images in a 78-year-old woman with positive results for osteoporosis at DXA and biomechanical CT analysis and for fragile bone strength at the hip and spine. **(a)** DXA-equivalent BMD analysis of the virtually isolated proximal femur (top) shows the femoral neck and total hip regions of interest, and quantitative BMD analysis of the L1 vertebral trabecular bone (bottom) shows the elliptical region of interest. **(b)** Cut-out views of the finite element models of the left proximal femur and L1 vertebral body show the distribution of element-level bone material properties as derived from CT attenuation data. **(c)** Virtual deformation patterns for the femur under a sideways fall loading and for the vertebra under a uniform compressive overload show regions of simulated bone tissue failure. Plastic-like (gray) elements are included in the model to evenly distribute loads over the bone surfaces. White = unfailed tissue, red = most extensive failure.

fracture risk assessment tool calculator, while the latter represents standard clinical practice for identifying patients with more general “clinically defined” osteoporosis (26–29). We compared each of these two DXA classifications against two classifications from biomechanical CT analysis: one for BMD-defined osteoporosis and the other for either BMD-defined osteoporosis or fragile bone strength. Predetermined, validated threshold values for BMD and bone strength were used for these classifications (14,19,20,29). Clinically, any patient with osteoporosis or fragile bone strength is classified as having a high risk for fracture. In our reclassification analysis, we calculated values of

percent agreement (the proportion of cases with the same classification, either positive or negative), sensitivity, specificity, positive and negative predictive values, the Kappa statistic, and the prevalence of positive cases; the Wilson score method was used to calculate a 95% confidence interval (CI) for sensitivity and specificity (30). All analyses were performed with JMP version 5.0 software (SAS Institute, Cary, NC).

Results

Biomechanical CT analysis was successfully completed at the hip for all women who underwent hip DXA ($n = 136$) and at the spine for all but one woman who

underwent spine DXA ($n = 106$, excluding the woman with a vertebral fracture in L1, L2, and L3). Overall, eight of 136 women with hip DXA had osteoporosis at the femoral neck (prevalence, 5.9%). For all women who underwent DXA at both the femoral neck and lumbar spine ($n = 107$), a comparison of the T scores for these sites identified only six women with osteoporosis at the femoral neck, 30 women with osteoporosis at the lumbar spine, and the same 30 women with clinically defined osteoporosis (at the femoral neck, total hip, or lumbar spine) (Fig 2). The correlation between the T scores at both sites was low ($R^2 = 0.36$), a paired t test showed a significant bias in the T-scores that

Figure 2

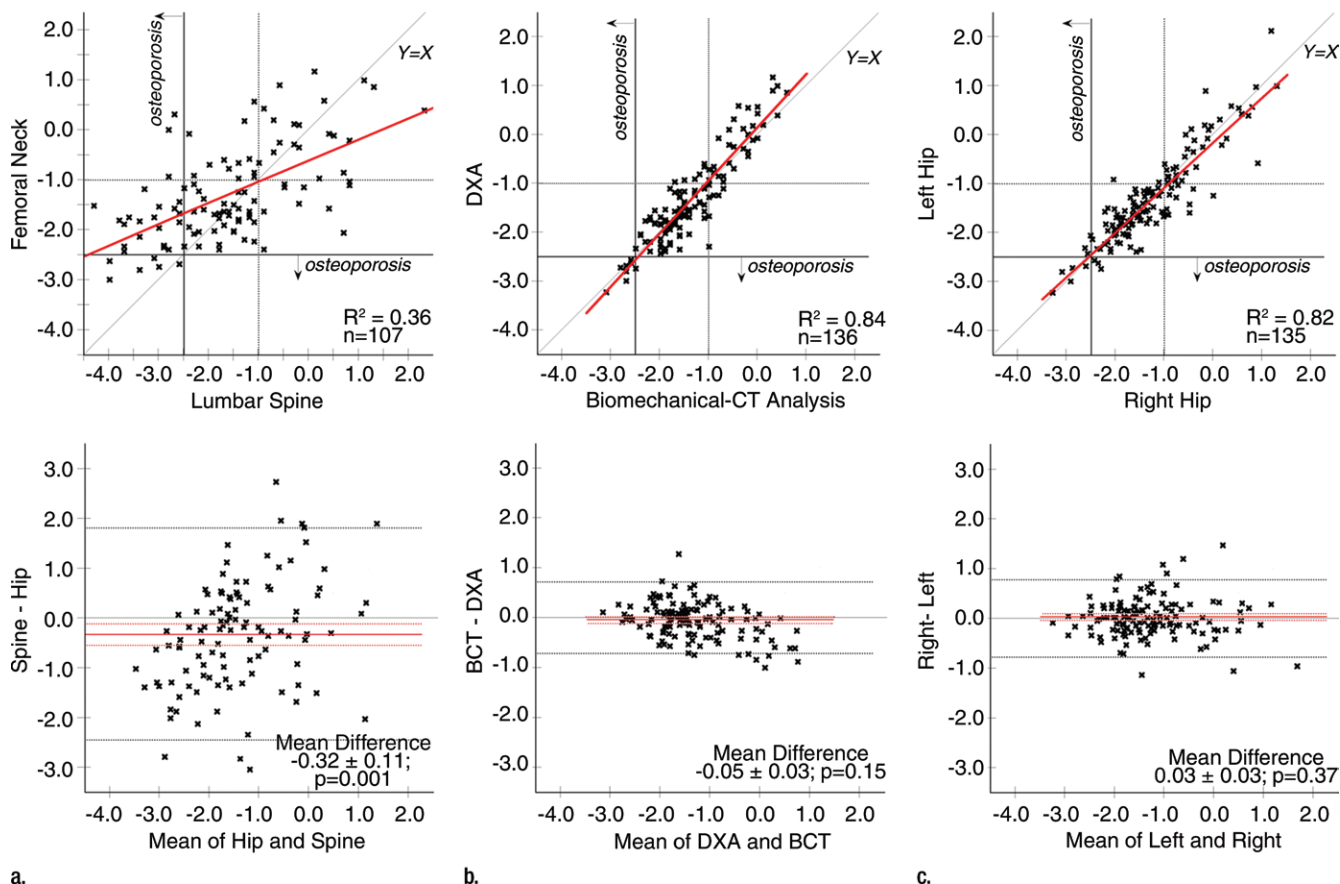


Figure 2: (a) Regression analysis (top) and corresponding Bland-Altman plot (bottom) shows comparison of DXA-measured BMD T scores (dimensionless units) at the femoral neck versus the lumbar spine ($n = 107$ women with DXA at both the hip and spine). (b) Regression analysis (top) and corresponding Bland-Altman plot (bottom) shows comparison of BMD T scores at the femoral neck for DXA versus biomechanical CT analysis ($n = 136$ women). (c) Regression analysis (top) and corresponding Bland-Altman plot (bottom) shows comparison of DXA-measured BMD T scores at the femoral neck for the left versus right femurs ($n = 135$ women with DXA at both the left and right hips). For regression plots, red line = least-squares best fit, solid black line = BMD T-score thresholds for osteoporosis, dashed black line = BMD T-score thresholds for osteopenia. The $Y = X$ line of unity is shown for reference. For Bland-Altman plots, solid red line = mean difference (bias) between the two measurements, dashed red lines = 95% CIs for that difference, dashed black lines = limits of agreement between the two measurements.

was -0.32 units lower for the spine ($P = .001$), and the corresponding Bland-Altman analysis displayed appreciable scatter, with the limits of agreement spanning -2.45 – 1.81 T-score units.

Directly comparing the T scores at the femoral neck between DXA and biomechanical CT analysis revealed good agreement. There was a high correlation ($R^2 = 0.84$), the mean difference of 0.05 T-score units (95% CI: -0.10 , 0.016) was not statistically different than zero ($P = .15$), and the limits of agreement were ± 0.71 T-score units. For reference, these trends were similar to those between the left- and

right-hip BMD T-scores as measured with only DXA: $R^2 = 0.82$; nonsignificant mean paired difference, 0.03 T-score units (95% CI: -0.037 , 0.098 ; $P = .37$); and limits of agreement, ± 0.78 T-score units. Bland-Altman analysis also revealed a slight downward trend for the DXA versus biomechanical CT differences at higher T-score values (T greater than -0.5). Further analysis revealed that this difference was positively but weakly correlated with body mass index ($R^2 = 0.07$; $P < .002$), with DXA values trending slightly higher than biomechanical CT values at higher T-score values. There were no significant trends

between body mass index and either left minus right differences in the DXA hip T scores or individual DXA or biomechanical CT T scores.

Overall agreement between osteoporosis classifications at the femoral neck provided by DXA and biomechanical CT analysis was 98.5%, with 134 of 136 women having the same positive or negative classification for osteoporosis at the femoral neck. The T scores in two women with different classifications were only differed by 0.2 units. Reclassification for osteoporosis at the femoral neck versus DXA as the reference was excellent, with high sensitivity (100%)

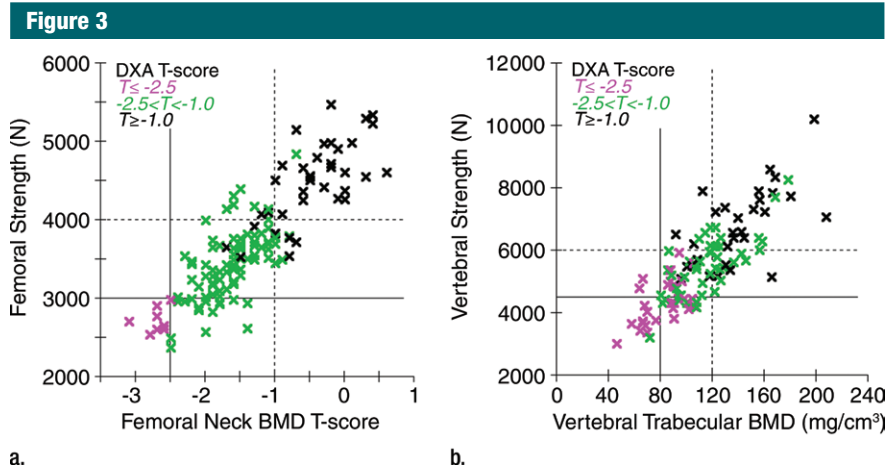


Figure 3: (a) Results from biomechanical CT analysis at the hip show femoral strength and the femoral neck BMD T score ($n = 136$). (b) Results from biomechanical CT analysis at the spine show spine strength and vertebral trabecular BMD ($n = 106$). Purple points = DXA-defined osteoporosis ($T\text{-score} \leq -2.5$), green points = patients with DXA-defined osteopenia ($-2.5 < T\text{-score} < -1.0$), solid vertical line = BMD T-score threshold for osteoporosis, dashed vertical line = BMD T-score threshold for osteopenia, solid horizontal line = strength threshold for fragile bone strength, dashed horizontal line = strength threshold for low bone strength.

in eight of eight patients (95% CI: 67.6, 100) and high specificity (98.4%) in 126 of 128 patients (95% CI: 94.5, 99.6) and a Kappa score of 0.88.

All eight of the women with osteoporosis at the femoral neck at DXA also had fragile bone strength at the hip at biomechanical CT analysis (Fig 3). In addition, 14 other women with fragile bone strength did not have osteoporosis at the femoral neck at DXA. The overall prevalence of fragile bone strength at the hip was 16.2% (22 of 136 women).

Considering both the hip and spine, agreement in diagnostic classification between DXA and biomechanical CT analysis was 84.9% (24 of 29 patients), with high sensitivity (82.8%) in 24 of 29 patients (95% CI: 65.4, 92.4) and high specificity (85.7%) in 66 of 77 patients (95% CI: 76.2, 91.8) (Table). Overall, in 90 of 106 women who underwent both hip and spine DXA, the same classification (ie, a positive or negative result) for clinically defined osteoporosis was the same at both DXA and biomechanical CT analysis, as was the result of biomechanical CT analysis for having a high risk for fracture (either osteoporosis or fragile bone strength). Of the 29 women who had positive

results for clinically defined osteoporosis at DXA, 24 also had positive results for having a high risk for fracture at biomechanical CT analysis, and of the 35 women who had positive results at biomechanical CT analysis, 11 had negative results at DXA. In the latter group of women, most of the discrepancy was due to classification differences at the spine. For example, eight women with either fragile bone strength or osteoporosis at the spine at biomechanical CT analysis did not have spinal osteoporosis at DXA (Fig 3b). According to our ad hoc analysis of images obtained at the index (or L1) vertebral level, aortic calcification was seen in 48 of 135 patients (35.6%), osteophytes were seen in 11 of 135 (8.1%), and degenerative changes in the facet joints were seen in three of 135 (2.2%) (Fig 4).

Discussion

In development in academia for over 20 years, biomechanical CT analysis provides arguably the most comprehensive available clinical assessment of bone integrity of the hip and spine (13,31). Previously, others established the utility of quantitative CT by using

an external calibration phantom to provide DXA-equivalent measures of hip BMD (14,16,32). By using clinical CT colonography images, we found excellent agreement between BMD and osteoporosis classifications between DXA, the current clinical standard, and biomechanical CT analysis without the use of any external calibration phantom. From both tests, BMD T scores at the hip were highly correlated with each other and had good absolute agreement, which was manifested at biomechanical CT analysis as having high sensitivity and specificity compared with DXA for depicting osteoporosis at the hip. Agreement between DXA and biomechanical CT analysis was as good as that between DXA of the spine and hip and between DXA of the left and right femurs. In addition, biomechanical CT analysis provides measures of trabecular BMD at the spine and measures of bone strength at the hip and spine. With these and hip BMD measurements, classifications of patients at high risk for general osteoporotic fracture also agreed well with the corresponding classifications of clinical osteoporosis at the hip or spine as defined by DXA.

We are aware of only one other study (Weber et al [15]) that compared biomechanical CT analysis with DXA with the use of clinical CT images and without an external calibration phantom, and our current results are consistent with those of that study. In the study by Weber et al, which used the same analysis software as we did, biomechanical CT analysis of the hip was applied to CT enterography images, which were obtained with intravenous contrast enhancement in 136 women and men with inflammatory bowel disease and spanned a wide age range (15). As in the current study, the DXA- and CT enterography-generated BMD T-score values at the hip were highly correlated ($R^2 = 0.84$), there was excellent absolute agreement in T scores, and, by using DXA as the reference, there was high sensitivity (85.7%) and specificity (98.5%) for classifying hip osteoporosis at biomechanical CT analysis. Spine analysis was not performed in the study by Weber et al because the intravenous

Diagnostic Equivalence of DXA and Biomechanical CT Analysis

Characteristic	DXA Femoral Neck (<i>n</i> = 136)		DXA Clinical (<i>n</i> = 106)	
	Osteoporosis*	Osteoporosis* or FBS†	Osteoporosis‡	Osteoporosis‡ or FBS§
Agreement	98.5 (134/136)	89.7 (122/136)	85.8 (91/106)	84.9 (90/106)
Sensitivity¶	100 (8/8) [67.6, 100]	100 (8/8) [67.6, 100]	55.2 (16/29) [37.6, 71.6]	82.8 (24/29) [91.0, 99.3]
Specificity¶	98.4 (126/128) [94.5, 99.6]	89.1 (114/128) [82.5, 93.4]	97.4 (75/77) [91.0, 99.3]	85.7 (66/77) [76.2, 91.8]
PPV	80.0 (8/10)	36.4 (8/22)	88.9 (16/18)	68.6 (24/35)
NPV	100 (126/126)	100 (114/114)	85.2 (75/88)	93.0 (66/71)
Kappa score**	0.88 ± 0.08	0.49 ± 0.11	0.60 ± 0.09	0.64 ± 0.08
BCT prevalence	7.4 (10/136)	16.2 (22/136)	17.0 (18/106)	33.0 (35/106)
DXA prevalence	5.9 (8/136)	...	27.4 (29/106)	...

Note.—Unless otherwise indicated, data are percentages, and data in parentheses are proportions. By using DXA-defined osteoporosis as the reference, classifications of osteoporosis at DXA were compared with those of osteoporosis at biomechanical CT or of osteoporosis or fragile bone strength at biomechanical CT. BCT = biomechanical CT analysis, FBS = fragile bone strength, NPV = negative predictive value, PPV = positive predictive value.

* Osteoporosis is defined as a T score ≤ -2.5 at the femoral neck.

† Fragile bone strength is defined as a femoral strength ≤ 3000 N.

‡ Osteoporosis is defined as a T score ≤ -2.5 at the femoral neck or total hip or a BMD ≤ 80 mg/cm³ at the spine.

§ Fragile bone strength is defined as a femoral strength ≤ 3000 N or a vertebral strength ≤ 4500 N.

¶ Data in brackets are 95% CIs.

** Data are Kappa score \pm standard error.

contrast agent permeates the highly porous and well vascularized vertebral trabecular bone, increasing its apparent attenuation, which, in turn, leads to overestimation of BMD measurement for that site (15,33).

Others have proposed that ancillary analysis of CT images be performed for opportunistic assessment of osteoporosis (9–12,34). Pickhardt et al (9) used both a phantomless calibration scheme and uncalibrated values of attenuation measured on spine-containing images to screen for patients at high risk for DXA-defined osteoporosis or a prevalent vertebral fracture; they later reported that the use of uncalibrated values is preferred because of the poor precision of their phantomless approach (11). Summers et al (10) reported a similar strategy that focused on CT colonography images and used a highly automated algorithm in which Hounsfield units were converted to units of BMD by using measurements obtained from prior patients. Mueller et al (12) used a phantomless calibration technique that used measurements made in muscle and fat. All these studies demonstrated the potential utility of ancillary analysis but only addressed

the spine, whereas one recent study addressed the hip (34).

In our study, we assessed the hip in addition to the spine. This is important because, compared with the spine, measurements made at the hip better identify patients who are at high risk for hip fracture, which is the most devastating consequence of osteoporosis (24). In addition, we provided measures of bone strength, enabling us to assess for fracture risk by using measures other than BMD. Although bone strength as a measure of risk is not yet clinically established, multiple large prospective fracture-outcome studies confirmed that these types of bone strength measures are highly associated with the incident risk of new hip and spine fractures in both women and men, with the risk association being at least as high as that for BMD (14,22,23,32,35–39). Other strengths of our study are that the phantomless calibration technique was not tuned in any way to the study data, and the overall analysis procedure had high repeatability precision (Appendix E1 [online]) (15). In general, calibration of CT attenuation data is important in measuring BMD because otherwise numeric values can be overly sensitive to

Figure 4

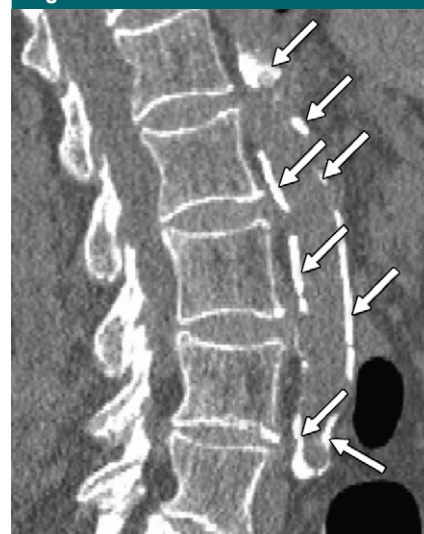


Figure 4: Sagittal section of L1–L5 vertebrae from a CT colonography image of an 85-year-old woman shows appreciable aortic calcification (arrows), which contributed to discrepancies that caused the patient to just miss testing positive for spine osteoporosis at DXA (T = -2.4); however, she definitively tested positive for both spine osteoporosis (vertebral trabecular BMD, 71 mg/cm³) and fragile bone strength (vertebral strength, 3220 N) at biomechanical CT analysis.

drift in imager characteristics, settings such as current exposure and voltage, intermachine differences, and, potentially, patient characteristics such as body mass index.

While the hip BMD measurements from biomechanical CT analysis were designed to mimic those provided by DXA, that is not the case for the spine. The spinal BMD measurement in the biomechanical CT spinal analysis, which is based on well-established clinical guidelines, is a volumetric measure that focuses on only the trabecular bone within the vertebral body, whereas DXA uses a projectional “areal” measure that encompasses the entire vertebral body and all the posterior elements (19,20). As such, the DXA BMD measure is influenced by aortic mineralization—which we found to be common in this cohort—and other degenerative changes, whereas the DXA BMD measurement is not; the DXA-based BMD measurement is also influenced by bone size and high body mass index (18,40,41). Such differences may explain why the risk for vertebral fracture is more highly associated with CT-based measures of vertebral trabecular BMD than it is with DXA-based measures of spinal BMD (22,35,37,42,43).

Our study has several limitations, including its retrospective nature, the inclusion of only women, and its small sample size. The wide CIs of sensitivity and specificity for depicting DXA-defined osteoporosis primarily reflect the low number of patients with osteoporosis in our sample. Our interventional thresholds for bone strength were developed by using a primarily white cohort and, therefore, may not apply to demographics with a fundamentally different relation between BMD and bone strength, such as African Americans and Asians, whose bones can be differently sized than those of European descent. The bone strength estimates themselves do not directly apply to disease conditions associated with abnormal collagen or mineral, including osteogenesis imperfecta, Paget disease, osteomalacia, and fluorosis (44).

In summary, we found excellent agreement between BMD and osteoporosis

classifications between DXA, the current clinical standard, and biomechanical CT analysis of the hip and spine as applied to previously acquired CT colonography images. Implementing this extra analysis for CT colonography images can provide patients with a comprehensive clinical assessment of osteoporosis without requiring any change to the CT protocol.

Acknowledgment: Amgen, Eli Lilly, and Merck. The authors had control of the data and information submitted for publication, and, beyond O.N. Diagnostics, these study sponsors did not have a role in the design and conduct of the study; in the collection, management, analysis, and interpretation of the data; or in the preparation of the manuscript. TMK is a consulting Chief Science Officer for and has stock ownership in O.N. Diagnostics. DLK and DCL are full-time employees of and have equity interests in O.N. Diagnostics. All other authors report no conflicts of interest. We would like to thank the following individuals at Mayo Clinic for their help: Elizabeth Atkinson, Assistant Professor of Biostatistics, who reviewed and assisted with addressing the statistical issues raised by the reviewers; Lifeng Yu, Ph.D., Associate Professor of Medical Physics, who assisted with calculating dose data for the CT colonography images; and Chi Ma, Ph.D., who also assisted with calculating dose data for the CT colonography images.

Disclosures of Conflicts of Interest: **J.L.F.** Activities related to the present article: received a grant from O.N. Diagnostics. Activities not related to the present article: disclosed no relevant activities. Other activities: disclosed no relevant activities. **N.S.M.** disclosed no relevant activities. **S.K.** disclosed no relevant activities. **B.L.C.** Activities related to the present article: disclosed no relevant activities. Activities not related to the present article: received personal fees from Amgen and a grant from NPS Pharmaceuticals. Other activities: disclosed no relevant activities. **D.H.B.** disclosed no relevant activities. **D.L.K.** Activities related to the present article: grants from Amgen, Merck, Eli Lilly, and the National Institutes of Health. Activities not related to the present article: personal fees from O.N. Diagnostics. Other activities: patents pending and owns equity in O.N. Diagnostics. **D.C.L.** Activities related to the present article: grants from Amgen, Merck, Eli Lilly, and the National Institutes of Health. Activities not related to the present article: personal fees from O.N. Diagnostics. Other activities: disclosed no relevant activities. **T.M.K.** Activities related to the present article: grants from Amgen, Merck, Eli Lilly, and the National Institutes of Health. Activities not related to the present article: personal fees from Merck, Amgen, and Agnovos Healthcare. Other activities: patents pending, owns equity, and consulting Chief Science Officer at O.N. Diagnostics.

References

1. Curtis JR, Carbone L, Cheng H, et al. Longitudinal trends in use of bone mass measure-

ment among older americans: 1999-2005. *J Bone Miner Res* 2008;23(7):1061-1067.

- Zhang J, Delzell E, Zhao H, et al. Central DXA utilization shifts from office-based to hospital-based settings among medicare beneficiaries in the wake of reimbursement changes. *J Bone Miner Res* 2012;27(4):858-864.
- King AB, Fiorentino DM. Medicare payment cuts for osteoporosis testing reduced use despite tests' benefit in reducing fractures. *Health Aff (Millwood)* 2011;30(12):2362-2370.
- Lim LS, Hoeksema LJ, Sherin K; ACPM Prevention Practice Committee. Screening for osteoporosis in the adult U.S. population: ACPM position statement on preventive practice. *Am J Prev Med* 2009;36(4):366-375.
- Lim SY, Lim JH, Nguyen D, et al. Screening for osteoporosis in men aged 70 years and older in a primary care setting in the United States. *Am J Men Health* 2013;7(4):350-354.
- Berrington de González A, Mahesh M, Kim KP, et al. Projected cancer risks from computed tomographic scans performed in the United States in 2007. *Arch Intern Med* 2009;169(22):2071-2077.
- Mettler FA Jr, Bhargavan M, Faulkner K, et al. Radiologic and nuclear medicine studies in the United States and worldwide: frequency, radiation dose, and comparison with other radiation sources—1950-2007. *Radiology* 2009;253(2):520-531.
- Pickhardt PJ, Choi JR, Hwang I, et al. Computed tomographic virtual colonoscopy to screen for colorectal neoplasia in asymptomatic adults. *N Engl J Med* 2003;349(23):2191-2200.
- Pickhardt PJ, Lee LJ, del Rio AM, et al. Simultaneous screening for osteoporosis at CT colonography: bone mineral density assessment using MDCT attenuation techniques compared with the DXA reference standard. *J Bone Miner Res* 2011;26(9):2194-2203.
- Summers RM, Baecher N, Yao J, et al. Feasibility of simultaneous computed tomographic colonography and fully automated bone mineral densitometry in a single examination. *J Comput Assist Tomogr* 2011;35(2):212-216.
- Pickhardt PJ, Pooler BD, Lauder T, del Rio AM, Bruce RJ, Binkley N. Opportunistic screening for osteoporosis using abdominal computed tomography scans obtained for other indications. *Ann Intern Med* 2013;158(8):588-595.
- Mueller DK, Kutscherenko A, Bartel H, Vlasenbroek A, Ourednicek P, Erckenbrecht J. Phantom-less QCT BMD system as screening tool for osteoporosis without additional radiation. *Eur J Radiol* 2011;79(3):375-381.

13. Keaveny TM. Biomechanical computed tomography-noninvasive bone strength analysis using clinical computed tomography scans. *Ann N Y Acad Sci* 2010;1192:57–65.
14. Kopperdahl DL, Aspelund T, Hoffmann PF, et al. Assessment of incident spine and hip fractures in women and men using finite element analysis of CT scans. *J Bone Miner Res* 2014;29(3):570–580.
15. Weber NK, Fidler JL, Keaveny TM, et al. Validation of a CT-derived method for osteoporosis screening in IBD patients undergoing contrast-enhanced CT enterography. *Am J Gastroenterol* 2014;109(3):401–408.
16. Khoo BC, Brown K, Cann C, et al. Comparison of QCT-derived and DXA-derived areal bone mineral density and T scores. *Osteoporos Int* 2009;20(9):1539–1545.
17. Johnson CD, Chen MH, Toledano AY, et al. Accuracy of CT colonography for detection of large adenomas and cancers. *N Engl J Med* 2008;359(12):1207–1217.
18. Tenne M, McGuigan F, Besjakov J, Gerdhem P, Åkesson K. Degenerative changes at the lumbar spine—implications for bone mineral density measurement in elderly women. *Osteoporos Int* 2013;24(4):1419–1428.
19. Engelke K, Adams JE, Armbrrecht G, et al. Clinical use of quantitative computed tomography and peripheral quantitative computed tomography in the management of osteoporosis in adults: the 2007 ISCD Official Positions. *J Clin Densitom* 2008;11(1):123–162.
20. ACR-SPR-SSR Practice Parameter for the Performance of Quantitative Computed Tomography (QCT) Bone Densitometry. American College of Radiology. Resolution 39. Amended 2014. <http://www.acr.org/~media/DE78D-218C7A64526A821A9E8645AB46D.pdf>. Accessed February 24, 2015.
21. Crawford RP, Cann CE, Keaveny TM. Finite element models predict in vitro vertebral body compressive strength better than quantitative computed tomography. *Bone* 2003;33(4):744–750.
22. Melton LJ 3rd, Riggs BL, Keaveny TM, et al. Structural determinants of vertebral fracture risk. *J Bone Miner Res* 2007;22(12):1885–1892.
23. Orwoll ES, Marshall LM, Nielson CM, et al. Finite element analysis of the proximal femur and hip fracture risk in older men. *J Bone Miner Res* 2009;24(3):475–483.
24. Kanis JA, McCloskey EV, Johansson H, Oden A, Melton LJ 3rd, Khaltaev N. A reference standard for the description of osteoporosis. *Bone* 2008;42(3):467–475.
25. Watts NB, Leslie WD, Foldes AJ, Miller PD. 2013 International Society for Clinical Densitometry Position Development Conference: Task Force on Normative Databases. *J Clin Densitom* 2013;16(4):472–481.
26. Kanis JA, Johnell O, Oden A, Johansson H, McCloskey E. FRAX and the assessment of fracture probability in men and women from the UK. *Osteoporos Int* 2008;19(4):385–397.
27. Fracture Risk Calculator. World Health Organization. <http://www.shef.ac.uk/FRAX>. Accessed May 27, 2014.
28. Baim S, Binkley N, Bilezikian JP, et al. Official Positions of the International Society for Clinical Densitometry and executive summary of the 2007 ISCD Position Development Conference. *J Clin Densitom* 2008;11(1):75–91.
29. Lewiecki EM, Gordon CM, Baim S, et al. International Society for Clinical Densitometry 2007 Adult and Pediatric Official Positions. *Bone* 2008;43(6):1115–1121.
30. Newcombe RG. Two-sided confidence intervals for the single proportion: comparison of seven methods. *Stat Med* 1998;17(8):857–872.
31. Engelke K, Libanati C, Fuerst T, Zysset P, Genant HK. Advanced CT based in vivo methods for the assessment of bone density, structure, and strength. *Curr Osteoporos Rep* 2013;11(3):246–255.
32. Keyak JH, Sigurdsson S, Karlsdottir G, et al. Male-female differences in the association between incident hip fracture and proximal femoral strength: a finite element analysis study. *Bone* 2011;48(6):1239–1245.
33. Bauer JS, Henning TD, Müller D, Lu Y, Majumdar S, Link TM. Volumetric quantitative CT of the spine and hip derived from contrast-enhanced MDCT: conversion factors. *AJR Am J Roentgenol* 2007;188(5):1294–1301.
34. Wang X, Sanyal A, Cawthon PM, et al. Prediction of new clinical vertebral fractures in elderly men using finite element analysis of CT scans. *J Bone Miner Res* 2012;27(4):808–816.
35. Faulkner KG, Cann CE, Hasegawa BH. Effect of bone distribution on vertebral strength: assessment with patient-specific nonlinear finite element analysis. *Radiology* 1991;179(3):669–674.
36. Melton LJ 3rd, Riggs BL, Keaveny TM, et al. Relation of vertebral deformities to bone density, structure, and strength. *J Bone Miner Res* 2010;25(9):1922–1930.
37. Imai K, Ohnishi I, Matsumoto T, Yamamoto S, Nakamura K. Assessment of vertebral fracture risk and therapeutic effects of alendronate in postmenopausal women using a quantitative computed tomography-based nonlinear finite element method. *Osteoporos Int* 2009;20(5):801–810.
38. Anderson DE, Demissie S, Allaire BT, et al. The associations between QCT-based vertebral bone measurements and prevalent vertebral fractures depend on the spinal locations of both bone measurement and fracture. *Osteoporos Int* 2014;25(2):559–566.
39. Ott SM, O'Hanlan M, Lipkin EW, Newell-Morris L. Evaluation of vertebral volumetric vs. areal bone mineral density during growth. *Bone* 1997;20(6):553–556.
40. Yu EW, Thomas BJ, Brown JK, Finkelstein JS. Simulated increases in body fat and errors in bone mineral density measurements by DXA and QCT. *J Bone Miner Res* 2012;27(1):119–124.
41. Guglielmi G, Grimston SK, Fischer KC, Pacifici R. Osteoporosis: diagnosis with lateral and posteroanterior dual x-ray absorptiometry compared with quantitative CT. *Radiology* 1994;192(3):845–850.
42. Yu W, Glüer CC, Grampp S, et al. Spinal bone mineral assessment in postmenopausal women: a comparison between dual X-ray absorptiometry and quantitative computed tomography. *Osteoporos Int* 1995;5(6):433–439.
43. Chavassieux P, Seeman E, Delmas PD. Insights into material and structural basis of bone fragility from diseases associated with fractures: how determinants of the biomechanical properties of bone are compromised by disease. *Endocr Rev* 2007;28(2):151–164.
44. Glüer CC, Blake G, Lu Y, Blunt BA, Jergas M, Genant HK. Accurate assessment of precision errors: how to measure the reproducibility of bone densitometry techniques. *Osteoporos Int* 1995;5(4):262–270.
45. Engelke K, Mastmeyer A, Bousson V, Fuerst T, Laredo JD, Kalender WA. Reanalysis precision of 3D quantitative computed tomography (QCT) of the spine. *Bone* 2009;44(4):566–572.
46. Lang TE, Li J, Harris ST, Genant HK. Assessment of vertebral bone mineral density using volumetric quantitative CT. *J Comput Assist Tomogr* 1999;23(1):130–137.
47. Pickhardt PJ, Bodeen G, Brett A, et al. Comparison of femoral neck BMD evaluation obtained using Lunar DXA and QCT with asynchronous calibration from CT colonography. *J Clin Densitom* 2015;18(1):5–12.